Proceedings of the 11th World Congress on Mechanical, Chemical, and Material Engineering (MCM'25)

Paris, France - August, 2025 Paper No. HTFF 165 DOI: 10.11159/htff25.165

# Experimental Characterization of Heat Transfer in a Partially Heated Rectangular Duct

## Md Arman Arefin<sup>1</sup>, Islam Ramadan<sup>1</sup>, Hélène Bailliet<sup>1</sup>

<sup>1</sup>Institut Pprime, University of Poitiers
Poitiers -86000, France
md.arman.arefin@univ-poitiers.fr; islam.ramadan@univ-poitiers.fr
helene.bailliet@univ-poitiers.fr

**Abstract** - This study aims to investigate the heat transfer characteristics of a partially heated rectangular duct. Understanding these characteristics can provide valuable insights into heat transfer in rectangular ducts commonly used in solar air heaters, plate heat exchangers, and similar geometrical configurations. Besides, there is no proper method in the literature to evaluate the heat transfer characteristics of such a configuration. Therefore, this study first develops a method and an experimental facility to evaluate the thermal characteristics. Extensive analysis was conducted to evaluate the validity of the system, and after being confirmed, thermal experiments were conducted. For evaluating the heat transfer behaviour, velocity and temperature profiles, and convective heat transfer coefficient are taken into consideration. Results suggest that the characteristics of heat transfer of a partially heated rectangular duct are unique and differ from those of flat plate and circular tube configurations.

**Keywords:** heated duct, heat transfer, boundary layer, heat transfer coefficient

#### 1. Introduction

A clear understanding of heat transfer characteristics in various geometrical configurations is crucial for optimizing thermal systems. While extensive studies have focused on circular ducts and flat plates, heat transfer in rectangular ducts - particularly partially heated ones - remains underexplored despite its engineering significance. One direct application of partially heated rectangular ducts is in modern solar air heaters, which are flat plate collectors used for heating air in household and industrial applications, such as space heating, crop drying, and wood seasoning [1]. However, a major challenge with these devices is their low efficiency due to inadequate convection between the air and the absorber plate [2], highlighting the need to better understand heat transfer characteristics from the surface to the air. Further, the concept of partially heated rectangular ducts is also employed in modern heat exchangers [3]. The development and optimization of these systems rely on a deeper understanding of the aerodynamic and heat transfer characteristics of partially heated rectangular ducts. Moreover, from an academic perspective, fully and partially heated rectangular ducts remain insufficiently studied. Besides, in many cases, the temperature distribution of rectangular ducts is considered analogous to that of a flat plate [4], though experimental validation of this consideration is lacking.

To address these gaps, an experimental method was developed to examine and evaluate the heat transfer process in a partially heated rectangular duct. Boundary layer development and the convective heat transfer coefficient are analyzed, and the results are compared with flat plates and circular ducts to better understand the specificity of the heat transfer behaviour of partially heated rectangular ducts.

## 2. Experimental setup and validation

As shown in Fig. 1, the experimental setup consists of a 2.6m long square duct made of aluminum that has a side length of 44 mm. The central part of the duct is replaced by a duct made of Plexiglas (having the same cross-section) to minimize the heat losses by conduction. Hereinafter, this part is referred to as the measurement section. The airflow is generated by a centrifugal fan (Model: FG351P9B) connected to one extremity of the duct via an 8m long circular flexible duct to mitigate the fan's vibrations and airflow fluctuations. The fan speed is controlled by a variable-speed motor. The airflow rate is measured by a flow meter placed at the downstream of the fan.

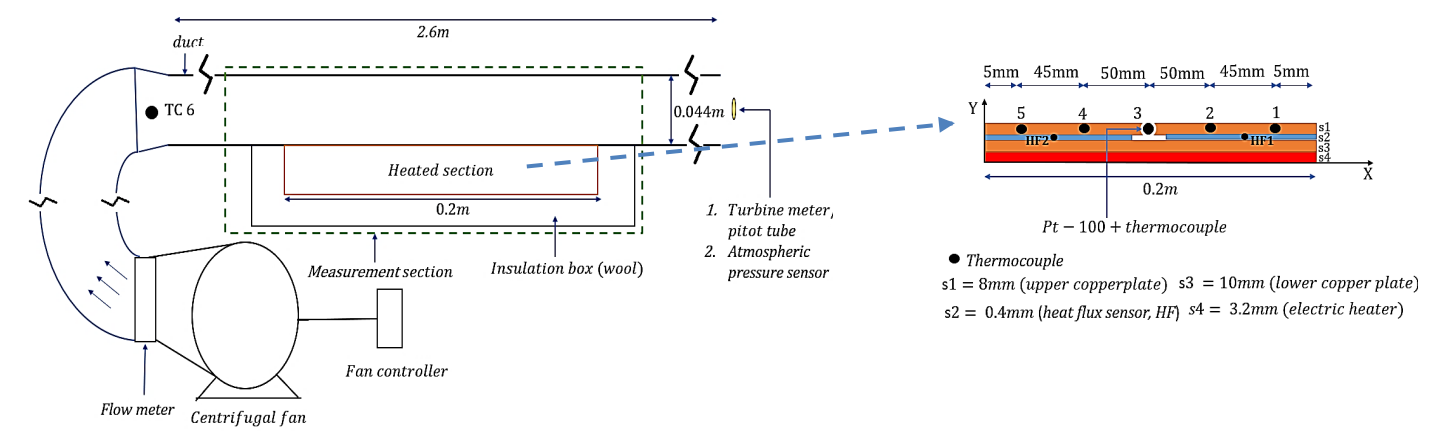


Fig 1: General schematic of the experimental setup (not to scale).

The mentioned circular pipe is connected to one end of the square duct with a circular-to-square adaptor. At this location, one thermocouple (number 6) is placed to measure the temperature of the incoming air. The bottom side of the duct in the measurement section is heated; this part is referred to as the heated section, where the top is a copper plate. There are five thermocouples inserted into the top copper plate at a distance of 4 mm from the upper surface of the plate (see Fig. 1). From the left of the copper plate, the thermocouples are placed at a distance (X) of 5, 50, 100, 150, and 195 mm, respectively. Further, below the copper plate, there are two heat flux sensors (Model: FHF05), which measure the heat flow conducted in the upper copper plate. Below the heat flux sensors, another copper plate of 10 mm thickness is placed to maintain the uniformity of heat coming from the heater positioned further below. A PID temperature controller (RB100 class) is used to control the heated wall temperature (measured by a pt100 sensor) via adjusting the electrical power supply to the heater. Hereinafter, the plate temperature is referred to as the solid temperature ( $T_s$ ). The pt-100 temperature sensor is inserted into the top copper plate in front of thermocouple number 3.

First, the uniformity of the top copper surface (without air flow) was assessed using a thermal camera. To perform these measurements, the upper side of the rectangular duct was removed. The temperature distribution of the top copper plate was evaluated alongside synchronized measurements from heat flux sensors to monitor the heat flux, while the temperatures of the five thermocouples were recorded to correlate between the infrared energy measured by the camera and the temperature. The thermal camera (Flir SC7000) was positioned vertically, focusing on the top copper plate. An integration time of 200 microseconds was chosen (optimal for temperatures between 11°C to 55°C) with a sampling frequency of 1 Hz. The results show that the steady state is reached after 1000 seconds of starting the heater and that the plate temperature is uniform with a maximum spatial temperature inhomogeneity of 0.1 °C, 0.9 °C, and 1°C for solid temperatures (*Ts*) of 30 °C, 40 °C, and 50 °C, respectively.

For the measurements, the system was first turned on by setting the desired temperature (i.e. solid temperature) on the PID controller. Then, the fan was activated, and the desired flow rate was set. Once the system reached a steady state, measurements were initiated. Collected data, acquired via a data acquisition system, were stored on a computer for further post-processing. To characterize the flow regime, velocity profiles were first measured using hot wire at an axial position (X) of 100 mm and at the duct entrance for Reynolds number Eq. (1) of 1500 and 6200. Then, temperature profiles were recorded at five different axial locations (corresponding to the thermocouple positions), and the thermal boundary layer thickness was determined. The vertical position of both the hot wire and the thermocouple was controlled using a vertical displacement system. Finally, the convective heat transfer coefficient was determined for varying Reynolds number.

$$Re = \frac{UD_h}{V},\tag{1}$$

where U is cross-sectional average velocity,  $D_h$  is the hydraulic diameter, and v is kinematic viscosity.

## 3. Results and discussion

In our setup, the transition from a laminar regime occurred at a Reynolds number of 4200. Fig. 2 shows the measured velocity profiles (in the lower half of the duct) at Reynolds number 1500 (laminar) and 6200 (turbulent) at ambient and 30°C (with and without heating). These profiles were obtained for an axial position (X) of 100 mm. The experimental measurements are in agreement with the analytical parabolic and 1/7<sup>th</sup> power law profiles for laminar and turbulent cases, respectively. A slight increase in velocity is also evident due to heating. It is predicted to occur partially due to the change in the density of air, and also to changes of the hot wire sensitivity due to temperature variations. Here, the sensitivity was set using the modified Kings law (or power law) using the below Eq. (2) [5].

$$E^2 = A + BU^n, (2)$$

where E is the voltage and U is the velocity of flow.

Figure 3 (where  $T_{\infty}$  is freestream temperature) shows the temperature profiles of the airflow at five different axial locations for a solid temperature ( $T_s$ ) of 30°C. The first point of the temperature profile was measured at a vertical position (Y) of 0.1 mm. Up to a vertical distance of 2 mm, 20 points were measured (i.e. vertical step of 0.1 mm). Then, the step was increased to 0.25 mm. It is evident from Fig. 3 that an effect of change in the flow regime is present on the temperature profiles. The thermal boundary layer thickness was estimated from the measured temperature profiles. Fig. 4 shows the thermal boundary layer thickness for laminar and turbulent cases.

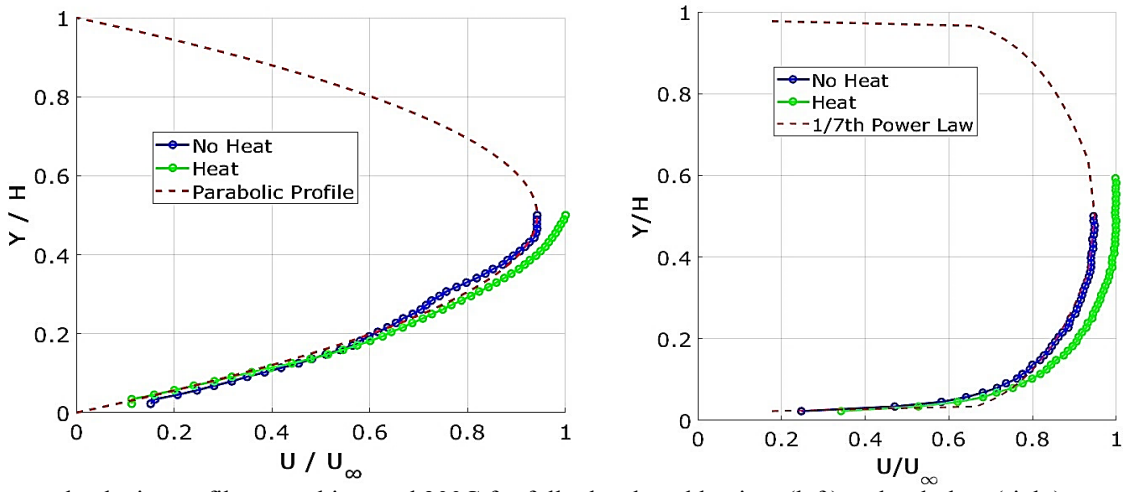


Fig 2: Measured velocity profiles at ambient and 300C for fully developed laminar (left) and turbulent (right) cases compared to analytical velocity profiles.

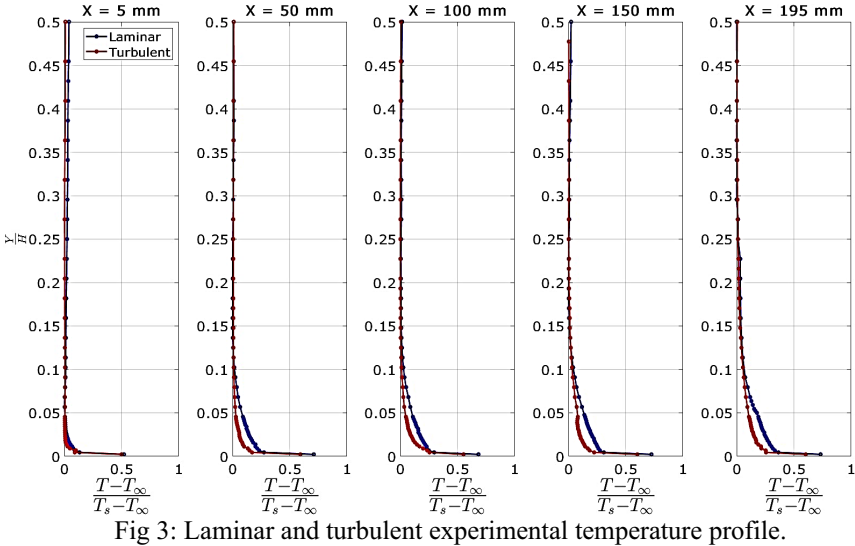
Finally, the evolution of the Nusselt number (Nu) with the Reynolds number was measured. The Nusselt number is calculated as follows:

$$Nu = \frac{hD_h}{K'},\tag{3}$$

where *K* is the thermal conductivity of gas taken as 0.264, 0.269, and 0.274  $W/m \cdot K$  respectively at temperatures of 30°C, 40°C, and 50°C, and *h* is the convective heat transfer coefficient, which is estimated as

$$h = \frac{q}{A\Delta T'} \tag{4}$$

where q is the heat transfer rate (W), A is the surface area of heat transfer  $(m^2)$ , and  $\Delta T$  is the temperature difference between the copper plate and free stream gas temperature  $(T_{\infty})$ .



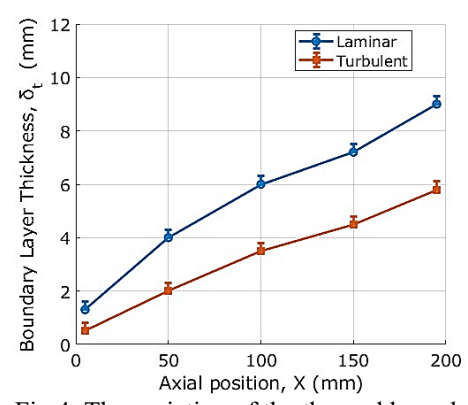
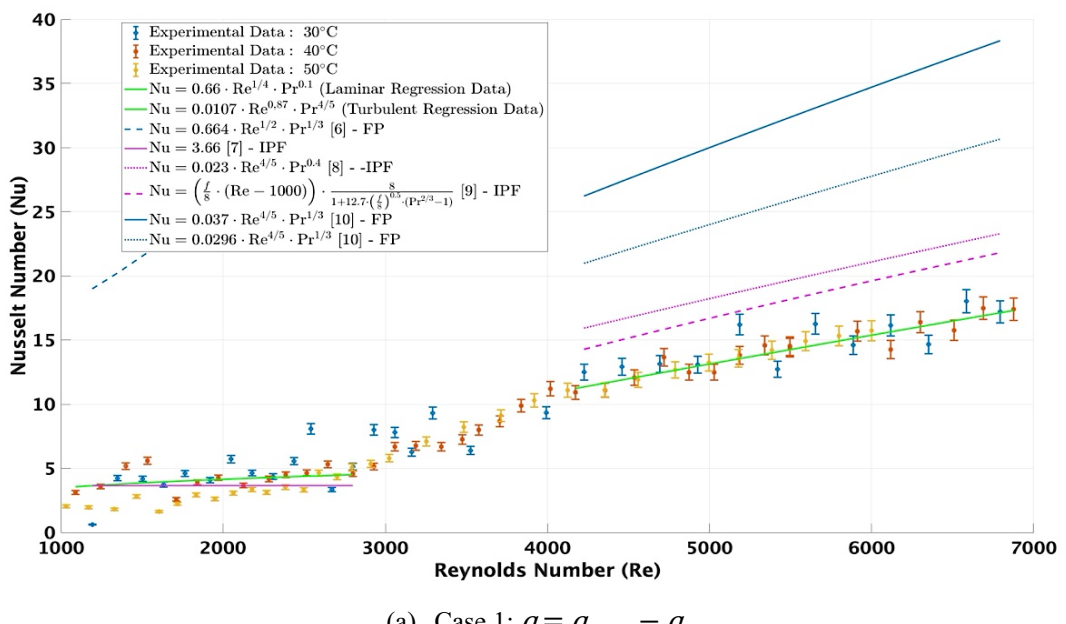


Fig 4: The variation of the thermal boundary layer thickness with the axial position over the heated plate for laminar and turbulent

For the calculation of q, two methods were applied: (1) considering heat loss, where the heat loss from the copper plate was considered and q was calculated using  $q = q_{total} - q_{loss}$ . Here,  $q_{total}$  is the value provided by the heat flux sensor in the presence of airflow at a certain solid temperature  $(T_s)$ , whereas  $q_{loss}$  is the value provided by the heat flux sensor (at the same  $T_s$ ) in the absence of the airflow, and (2) q is taken as  $q_{total}$ . Results obtained for Nu for both cases are provided in Fig. 5. The measurements were performed at three different solid temperatures ( $T_s$ ): 30°C, 40°C, and 50°C. The error bars are calculated based on uncertainty propagation. The measurement results are quite similar for the three solid temperatures. Besides, a comparison with different correlations found in the literature for flow through a pipe (purple curves in Fig 5) and over a flat plate (blue curves in Fig 5) shows that the convective heat transfer of a partially heated rectangular duct is different from that of a pipe or flat plate flow.



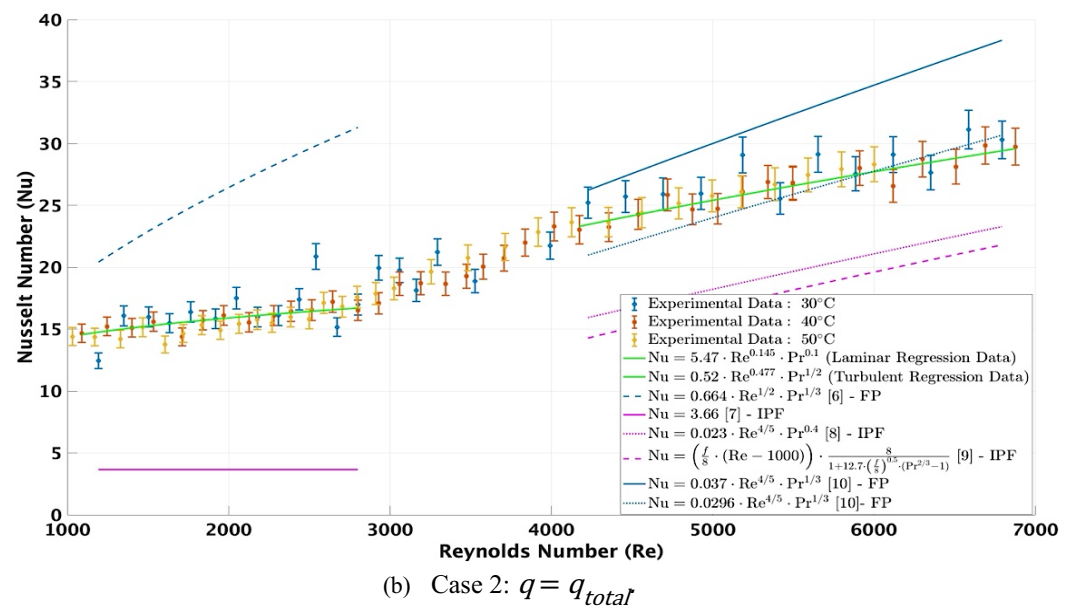


Fig 5: The evolution of the Nusselt number with Reynolds number for three different solid temperatures compared with previous works for both internal pipe flow (IPF) (purple curves) and flat plate (FP) (blue curves).

### 4. Conclusion

An experimental study was conducted to investigate heat transfer in a partially heated rectangular duct across different flow regimes. The evolution of the temperature profile and the thermal boundary layer thickness was analyzed. New correlations were developed, revealing that the Nusselt number evolution for this geometry differs from those reported in the literature for heated flat plates or circular ducts. This study can be used as a reference for describing heat transfer in solar air heaters, heat exchangers, and other engineering applications.

#### References

- [1] S. S. Patel and A. Lanjewar, "Experimental investigation of solar air heater duct with discrete V-rib integrated with staggered elements," Int. J. Sustain. Eng., vol. 14, no. 2, pp. 162–171, 2021.
- [2] H. Abulkhair, A. O. Alsaiari, I. Ahmed, E. Almatrafi, N. Madhukeshwara, and B. R. Sreenivasa, "Heat transfer and air flow friction in solar air heaters: A comprehensive computational and experimental investigation with wire-roughened absorber plate," Case Stud. Therm. Eng., vol. 48, p. 103148, 2023.
- [3] K. Karabulut, "Heat transfer and thermal-hydraulic evaluations of cross-circular grooved rectangular flow ducts depending on rectangular baffle design parameters," Eur. Phys. J. Plus, vol. 139, no. 3, p. 227, 2024.
- [4] Y. Zhang and M. Li, "Research on flow and heat transfer characteristics of heat transfer surface of trapezoidal duct," Heat Mass Transf., vol. 56, no. 5, pp. 1475–1486, 2020.
- [5] C. Norberg, Laboration 2b: Hot Wire Anemometry, 2009. [Online]. Available: https://www.lth.se/fileadmin/ht/Kursers/MMV211 /lab2b-pm-Eng-2009.pdf. Accessed: Dec. 17, 2024.
- [6] F. P. Incropera, D. P. DeWitt, T. L. Bergman, and A. S. Lavine, Fundamentals of Heat and Mass Transfer, 6th ed. New York, NY, USA: Wiley, 1996.
- [7] M. O. Hamdan, "Tapping to geothermal energy through a high-performance earth-to-water heat exchanger design," in 2018 5th International Conference on Renewable Energy: Generation and Applications (ICREGA), 2018, pp. 207–210.
- [8] I. Tosun, Modeling in Transport Phenomena: A Conceptual Approach. Amsterdam, Netherlands: Elsevier, 2007.
- [9] V. Gnielinski, "Neue Gleichungen für den Wärme-und den Stoffübergang in turbulent durchströmten Rohren und Kanälen," Forsch. Ingenieurwes. A, vol. 41, pp. 8-16, 1975.

| [10] Y. A. Çengel and A. J. Ghajar, Heat<br>McGraw-Hill Education, 2020. | and Mass Transfer: Fun | ndamentals and Application | ons, 6th ed. New York | , NY, USA: |
|--|------------------------|----------------------------|-----------------------|------------|
|  |                        |                            |                       |            |
|  |                        |                            |                       |            |
|  |                        |                            |                       |            |
|  |                        |                            |                       |            |
|  |                        |                            |                       |            |
|  |                        |                            |                       |            |
|  |                        |                            |                       |            |
|  |                        |                            |                       |            |
|  |                        |                            |                       |            |
|  |                        |                            |                       |            |
|  |                        |                            |                       |            |
|  |                        |                            |                       |            |
|  |                        |                            |                       |            |
|  |                        |                            |                       |            |